IEEE Access
Multidisciplinary | Rapid Review | Open Access Journal

Received January 6, 2020, accepted January 20, 2020, date of publication February 3, 2020, date of current version February 11, 2020.

Digital Object Identifier 10.1109/ACCESS.2020.2971314

Simulation on Current Density Distribution of Current-Carrying Friction Pair Used in Pantograph-Catenary System

GUO FENGYI, (Member, IEEE), GU XIN, WANG ZHIYONG, WANG YUTING, AND WANG XILI

Faculty of Electrical and Control Engineering, Liaoning Technical University, Huludao 125105, China

Corresponding author: Gu Xin (calista_gu@163.com)

The work was supported in part by the National Natural Science Foundation of China under Grant 51674136, in part by the Liaoning Revitalization Talents Program under Grant XLYC1802110, and in part by the Planned Project of Liaoning Natural Funds under Grant 2019-ZD-0034.

ABSTRACT Pantograph-catenary system is the key part of train current collection. The current density distribution of current-carrying friction pair used in pantograph-catenary system affects the safety running of train. At present, there is little research on the current density distribution of the friction pair. Because it is difficult to measure the current density directly, it is necessary to study by simulation. A sliding electrical contact simulation model of pantograph-catenary system was established by COMSOL Multiphysics software. The current density distribution of the friction pair under normal, light, and heavy rain conditions were studied with the simulation model. The current density isosurface in contact wire is saddle-shaped, and that in slide is arc-shaped. Under normal condition, the current density of contact area increases firstly and then decreases with the increase of contact force. It increases with the increase of current and decreases with the increase of sliding speed. Under rain condition, the current density decreases firstly and then increases with the increase of contact force. It increases with the increase of current. It increases firstly, then decreases and finally increases with the increase of sliding speed. Under the same contact force, sliding speed, and current conditions, the current density under rain condition is lower than that under no rain condition. Finally, the validity of the model was verified.

INDEX TERMS Current density, pantograph-catenary system, rain environment, sliding electrical contact.

I. INTRODUCTION

The pantograph-catenary system is an important part to ensure current collection performance of electric locomotive. The current density distribution of current-carrying friction pair used in pantograph-catenary system directly affects the temperature characteristics of contact area, and then affects the safety running of train.

The operating environment of pantograph-catenary system is relatively complex. Environment factor, operation speed, contact force and other factors have important influence on the amplitude and distribution of current density. If the current density of electrical contact point is too high, the local temperature will continuously rise, which will lead to failure of the electric contact performance and even burn the contact surface. Current density is regarded as a criterion for the occurrence of electric erosion [1]. Therefore, it is of great significance to analyze current density of the current-carrying friction pair used in pantograph-catenary system.

In recent years, current density and temperature of contact surface, contact resistance, and current collection quality of pantograph-catenary system have been studied. The current density distribution characteristics on the contact surface was obtained with semiconductor wafer experiments. As a result, it was confirmed that electric current was uniformly distributed over the contact area covered by an oxide film [2]. The size and location of conductive spot and surrounding conductive spots have a great influence on the current density of conductive spots [3]. It was shown that the current density distribution across the contact surface remains finite as compared to that of the idealized co-planar case [4]. The dynamic characteristics of the switching arc in different media were

The associate editor coordinating the review of this manuscript and approving it for publication was Giambattista Gruosso.

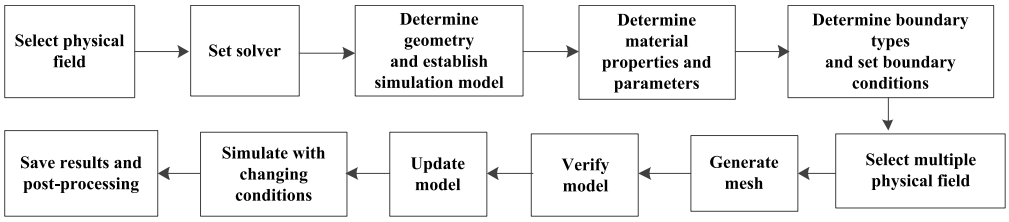

FIGURE 1. Flowchart of establishment of the simulation model.

analyzed, and the current density of the boundary between arc and electrode was studied [5]. They found that the conductive points distribute inside the indentation scar, which was mechanically fabricated on Sn-coated-Cu and Sn-bulk plates, and the resistance of conductive points dominated the total contact resistance [6]. A pantograph arc model was built to obtain the heat flux density injected into pantograph slide and the effect of operation speed on surface erosion of pantograph slide was studied [7]. The electromagnetic noise under the condition of arc in sliding electrical contact was studied [8]. The effect of current density on temperature and surface morphology was analyzed and the results showed that the higher the current density was, the higher the surface temperature was [9]. The effects of speed, contact force and spring stiffness on current collection quality of contact rail and collector shoe system were analyzed by considering the elasticity of catenary [10]. The thermoelectric characteristics of rough contact area was studied [11]. The current density distribution of pantograph arc was studied by using a magneto-hydrodynamic model. The arc column constricts and current density increases as the arc develops from cathode region to anode surface [12]. The transient process of contact surface temperature of a current-carrying friction pair used in pantograph-catenary system was simulated [13]. It showed that the temperature decreased from contact area to surrounding area. The contact force of pantograph-catenary system was evaluated and the influence of the friction coupling on the current collection was analyzed through the numerical simulation [14]. The influence mechanisms of operating speed, current, fluctuating amplitude and fluctuating frequency of compressive load on friction and wear rate were studied [15]. The results showed that increasing contact wire tension and decreasing messenger wire tension could improve the current collection quality between pantograph and catenary [16]. The influence of wind load on the dynamic interaction performance of pantograph-catenary was analyzed [17], [18].

Current researches mainly focus on arc current density and the relationship between temperature and current density. The most studies in the filed of pantograph-catenary are relevant to the dynamic interaction performance. The research on current density distribution of current-carrying friction pair used in pantograph-catenary system is relatively rare. Especially, research on current density and its influence factors of the friction pair under rain condition haven't been reported.

In this paper, a sliding electrical contact simulation model of pantograph-catenary system was established and its validity was verified by experiments. The current density distribution of the friction pair under different conditions was simulated and analyzed. The model does not consider the influence of wind load and other external disturbances. The current density characteristics of contact surface under no rain, light rain, and heavy rain conditions were compared. The effect of contact force, current, and sliding speed on current density was studied.

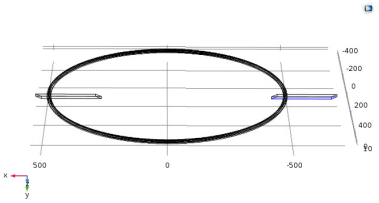

FIGURE 2. Geometric model.

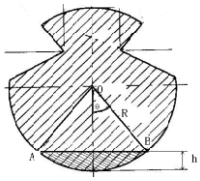

FIGURE 3. Cross section of contact wire.

II. SIMULATION MODEL

The sliding electrical contact simulation model was established by COMSOL Multiphysics software. The modeling process is shown in Fig. 1.

The established simulation model mainly revolves electric field and temperature field. The two physical fields interact with each other and affect the electrical contact state together. The modules of heat transfer, solid mechanics, and multi-body dynamics in COMSOL were mainly used to establish the simulation model.

A. ESTABLISHMENT OF GEOMETRIC SIMULATION MODEL

The three-dimensional geometric model was established according to the actual size of our experimental equipment. The contact wire was simulated by a circular copper wire, as shown in Fig. 2. Its main radius is 491mm and small radius R is 8mm. Considering the wear of contact wire during long-term experiments, the wear amount h was set to 1mm. The cross section of the contact wire is shown in Fig. 3. The contact wire moves in a circle on x-z plane and the contact

TABLE 1. Physical parameters of slide and contact wire.

Material	Thermal conductivity [W•(m•K)$^{-1}$]	Specific heat capacity [J•(kg•K)$^{-1}$]	Poisson ratio	Elasticity coefficient (Gpa)	Resistivity (Ω•m)	Density (kg•m^{-3})	Friction coefficient
Slide	15	660.2	0.425	12.6	8×10^{-6}	3.4×10^{3}	0.2
Contact wire	380	380	0.326	119	1.8×10^{-8}	8.9×10^{3}	0.2

TABLE 2. Material parameters of water.

Material	Surface emissivity	Poisson ratio	Density (kg•m^{-3})	Conductivity (S•m^{-1})	Specific heat capacity [J•(kg•K)$^{-1}$]	Thermal conductivity [W•(m•K)$^{-1}$]
Water	0.95	0.5	1.0×10^{3}	5.5×10^{-6}	4.2×10^{3}	0.6

slides move back and forth along x-axis direction to simulate zigzag motion between the contact line and contact slide.

B. DETERMINATION OF MATERIAL PARAMETERS

The material parameters of the slide and contact wire are shown in Tab. 1. In the simulation process, it is assumed that the material properties keep constant and the wear of materials is neglected. The convective heat dissipation of air is considered. The coefficient of heat dissipation is constant.

An adjustable water spray system was used to simulate rain environment. The system is mainly composed of a regulator and a pump. The heavy or light rain was simulated by controlling the amount of spraying water. It was achieved by adjusting the working voltage of the pump. According to IEC 60068 standard [19], the rainfall amount of light rain is 30g and the rainfall intensity is 60mm/h. The corresponding working voltage of the pump is 3.3V. The rainfall amount of heavy rain is 150g and the rainfall intensity is 300mm/h. The corresponding working voltage is 5.5V. In the simulation model, the rain condition was achieved by setting a layer of water film on the surface of the slide and contact wire. The material parameters of water are shown in Tab. 2.

C. BOUNDARY CONDITIONS

The temperature field constraints in the model are as follows:

The external forced convection was used as heat flux boundary. The convective heat transfer coefficient is related to the sliding speed of contact wire. The external temperature was set to 15°.

The electric field constraints in the model are as follows:

The system follows current conservation law. The governing equations are as follows:

$$\nabla \cdot J = Q_j \tag{1}$$

$$J = \left(\sigma + \varepsilon_0 \varepsilon_r \frac{\partial}{\partial t}\right) E + J_e \tag{2}$$

$$E = -\nabla V \tag{3}$$

Among them, σ is conductivity of the material. ε_r is relative dielectric constant. The current passing through the contact surface of the friction pair is the sum of the currents at multiple contact points.

$$n \cdot J = h_c \left(V_1 - V_2\right) \tag{4}$$

where h_c is contact surface conductance. J is contact surface current density. V_1 and V_2 are the two boundary potential of the contact surface respectively.

After the setup was completed, the transient solver was selected to simulate the model. The required simulation results were derived from the result module.

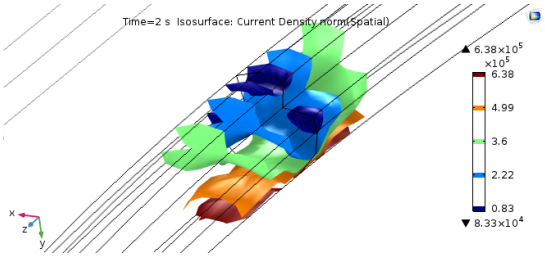

FIGURE 4. Isosurface distribution of current density norm in contact wire.

III. SIMULATION OF CURRENT DENSITY DISTRIBUTION

The distribution of current density in contact line and slide is represented by current density norm. It refers to the absolute value of current density.

A. ISOSURFACE DISTRIBUTION OF CURRENT DENSITY NORM IN CONTACT WIRE

When contact force is 60N, sliding speed is 20km/h, and contact current is 100A, the isosurface distribution of current density norm in contact wire is shown in Fig. 4. It shows the isosurface distribution is saddle-shaped.

In y-z plane, along the negative direction of y-axis, the two sides of the isosurface are higher and the middle is lower. That is, the isosurface far from contact surface is higher, while the one near the contact surface is lower, as shown in Fig. 5. The reason for this phenomenon is that the current line bends to both sides of the contact wire when it flows through the contact wire from the contact area. That is to say it bends from the negative direction of y-axis to the two sides of z-axis. The current density norm decreases gradually from the contact

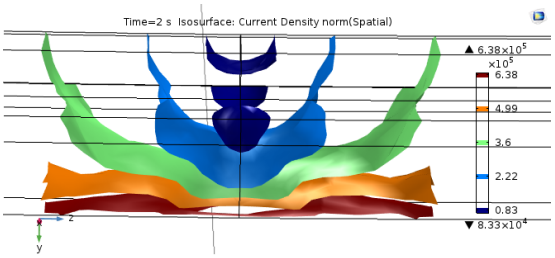

FIGURE 5. Isosurface distribution of current density norm in y-z plane.

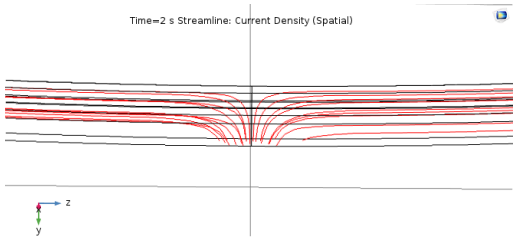

FIGURE 6. Streamline diagram of current density in contact wire.

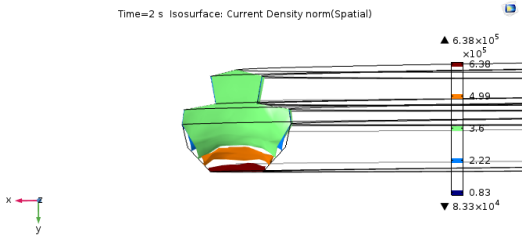

FIGURE 7. Isosurface distribution of current density norm in x-y plane.

surface to the contact wire. Because the contact area is small, the current is concentrated and the current density is large. While in the area far from the contact surface, the current line is sparse and the current density is small.

Fig. 6 is a streamline diagram of current density in contact wire. The current line is relatively dense near the contact area and it bends from the contact surface to both sides of z-axis.

In x-y plane, along the negative direction of z-axis, the middle of the isosurface is higher and the two sides are lower. That is, the isosurface near the center of the small radius of contact wire is higher, while the one at the edge of the conductor cross-section is lower, as shown in Fig. 7. This is mainly because the area of contact wire is larger than that of the contact surface, and the current conduction from inside of the contact wire to contact surface is a contraction process. So the current density is large in the middle of the same horizontal plane, and current density at the edge is small. The isosurface of current density norm is higher in the middle and that near two sides are lower.

B. ISOSURFACE DISTRIBUTION OF CURRENT DENSITY NORM IN SLIDE

Fig. 8 is the isosurface distribution of current density norm in slide under the same simulation condition as in Fig. 4. The farther away from the contact surface, the smaller the current density is. The isosurface near the contact surface is

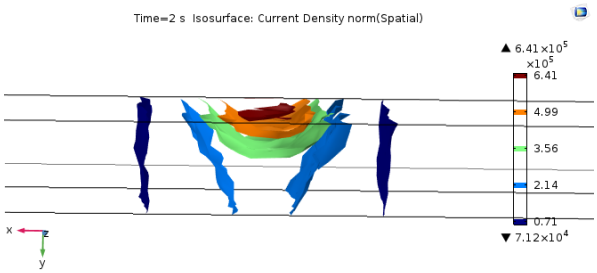

FIGURE 8. Isosurface distribution of current density norm in slide.

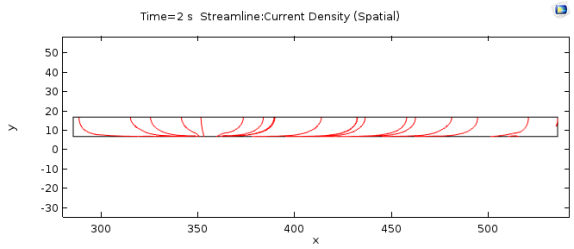

FIGURE 9. Streamline diagram of current density in slide.

arc-shaped. During the simulation, the potential was applied uniformly on the lower surface of the two slides. The lower surface doesn't contact with the contact wire. When current flows from the slide to contact surface, current lines concentrate and the current density is higher near the contact surface. The current density far from the contact wire is smaller.

In x-y plane, along the negative direction of z-axis, the current line bends from two sides of x-axis to negative direction of y-axis when it flows from slide to contact area, as shown in Fig. 9. The contact area is small, and the current lines varies from expansion to contraction. At the same horizontal plane, the current density far from the center the contact surface is smaller. Therefore, the isosurface of current density norm near the contact surface is arc-shaped.

IV. MAXIMUM CURRENT DENSITY OF THE CONTACT SURFACES

The maximum current density of the contact surface under different conditions is shown in Fig. 10.

When contact current is 200A and sliding speed is 120km/h, the maximum current density increases firstly and then decreases with the increase of contact force under no rain condition, as shown in Fig. 10 (a). However, the maximum current density decreases firstly and then increases with the increase of contact force under light and heavy rain conditions. The possible reasons for the above results are as follows. Under no rain condition, when contact force increases from 70N to 90N, the actual contact area increases, and it leads to the decrease of current density. On the other hand, the increase of friction heat leads to the increase of temperature. The relationship between temperature and contact voltage is as follows:

$$T_M^2 - T_0^2 = U_j^2/4L \tag{5}$$

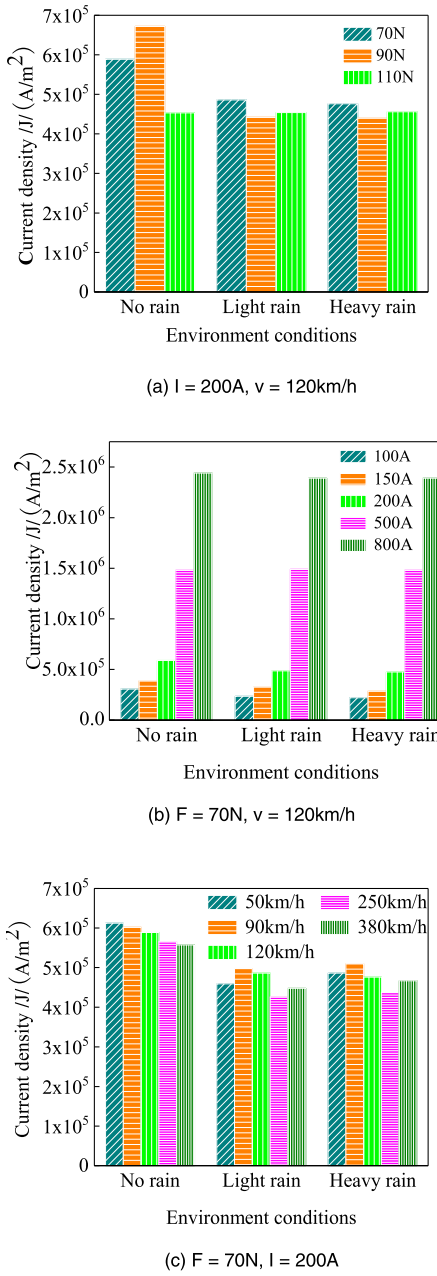

FIGURE 10. **Maximum current density of contact surface under different conditions.**

where T_0 is the temperature of the conductor outside the shrinkage area, T_M is the maximum temperature of the conductive spot. U_j is contact voltage. Lorentz coefficient is $L = 2.4 \times 10^{-8}(\mathrm{V/K})^2$.

According to formula (5), the contact voltage increases with the increased contact temperature. In that case, the contact resistance increases with a constant contact current according to Ohm's law. The friction pair of the machine is composed of copper impregnated carbon slide and copper contact wire. Copper oxide film and carbon film may be formed during the experiment, whose breakdown voltage is about 0.7V. The film can be broken down under the contact voltage of several volts. Therefore, there is no film resistance, only constriction resistance. Under the same contact condition, the increase of contact resistance (constriction resistance) means the decrease of actual contact area. Therefore, the current density increases with a constant current. So the current density increases because the later effect is more obvious. When contact force increases from 90N to 110N, the current density decreases due to increasing of actual contact area.

Under rain condition, water film is formed. When contact force increases from 70N to 90N, the lubrication of water improves the contact performance [20], [21], so the current density reduces. When contact force increases from 90N to 110N, the water film thickness becomes thin or even breaks down due to increased friction action. So the current density increases.

From Fig. 10 (a), we can see that the current density under no rain, light rain, and heavy rain conditions is almost the same when contact force is 110N. It indicates that the water film might break down. In this case, the water film has little effect on current density.

Fig. 10 (b) shows that the maximum current density always increases with the increase of contact current when contact force and sliding speed keep constant. Whether there is rain or not, the changing trend is the same.

Fig. 10 (c) shows that the maximum current density decreases with the increase of sliding speed under no rain condition. However, under rain condition, it increases firstly, then decreases and finally increases with the increase of sliding speed.

The possible reasons are as follows. Under no rain condition, the convective heat dissipation of air increases with the increase of sliding speed, so the temperature of contact surface decreases. According to formula (4) and (5), the contact voltage decreases with the decreased contact temperature. And the current density decreases with a constant current.

Under rain condition, on the one hand, the contact performance is improved due to the lubrication of water. On the other hand, the contact temperature decreases due to the heat dissipation action of rain. So the current density is smaller than that under no rain condition.

According to the thickness of water film, the lubrication state of water film belongs to thin film lubrication. In low speed range, because the film is thinner, an ordered liquid film is easy to form [21]. When the lubrication film is arranged from disorder to order, the lubrication effect becomes better, so the current density at 50km/h is the smallest. When sliding speed is 90km/h and 120km/h, the sliding speed is higher, and the ordered film is difficult to form. So the lubrication effect is not as good as that of at 50km/h, the current density increases. However, the heat dissipation at 120km/h is better than that of at 90km/h, so the current density at 120km/h is smaller than that at 90km/h. At 380km/h, the friction heat and the temperature is higher, so the current density is higher. Therefore, the maximum current density increases firstly, then decreases and finally increases with the increase of sliding speed.

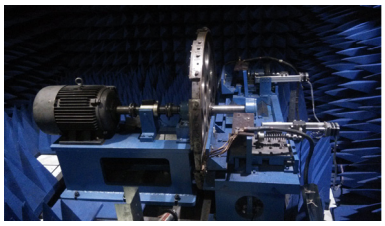

FIGURE 11. Sliding electrical contact experimental device.

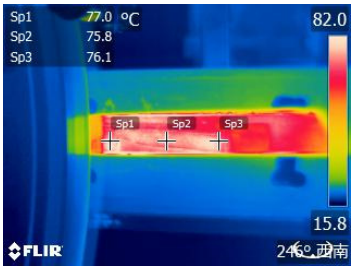

FIGURE 12. Measured contact temperature of the friction pair.

Comparing with Fig. 10 (a) - (c), it can be seen that under different conditions, the difference of influence of heavy rain and light rain on current density is small.

V. MODEL VERIFICATION

It is difficult to directly measure the current density of contact surface. There is a coupling relationship between the current density and the temperature. According to formula (4) and (5), when the temperature T_M increases, the contact voltage U_j increases. The current density increases when the contact voltage U_j increases. So the validity of the model can be indirectly verified by comparing the measured and simulated contact temperature.

The temperature experiment was carried out as follows:

A sliding electrical contact experimental device [22], as shown in Fig. 11, was used to complete the current-carrying characteristics experiments under different contact force, sliding speed, and contact current conditions. The friction pair of the machine is composed of copper impregnated carbon slide and copper contact wire. It can simulate train operation and adjust contact force, sliding speed, and contact current. The contact force, sliding speed, and contact current can be measured and stored by a Labview-based software. A FLIR-T400 type infrared thermal imager was used to collect the temperature of the contact zone of the slide.

The initial conditions are as follows: contact force is 70N, sliding speed is 120km/h, and contact current is 200A. Fig. 12 is the measured contact temperature of the friction pair taken by infrared thermal imager. Fig. 13 is the corresponding simulation result when simulation time is 600s. When contact force is 70N, sliding speed is 120km/h, and contact current is 200A, the comparison of contact temperature between experimental and simulation results under different rain conditions is shown in Fig. 14. The maximum error is 9.4%, and the simulation accuracy is satisfied. So the simulation model is valid.

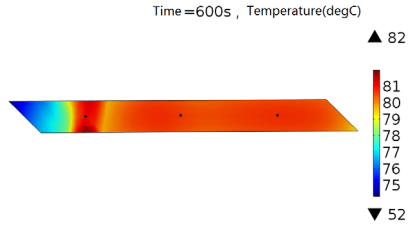

(a) Temperature Distribution of the Slide Contact Zone

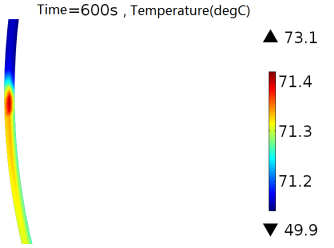

(b) Temperature Distribution of the Contact Area of Wire

FIGURE 13. Simulation results of temperature field.

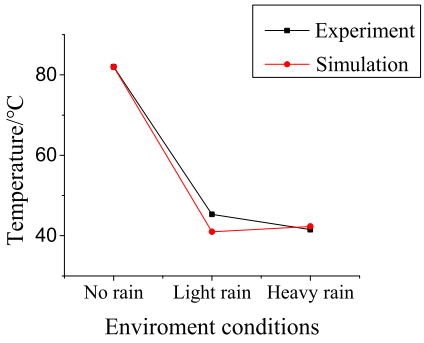

FIGURE 14. Contact temperature comparison under different rain conditions.

VI. CONCLUSION

1) The isosurface of current density norm in contact wire is saddle-shaped, while that of in slide is arc-shaped.

2) Under no rain condition, the maximum current density in contact surface increases firstly and then decreases with the increasing contact force. It increases with the increasing contact current and decreases with the increasing sliding speed.

3) Under rain condition, the maximum current density of contact surface decreases firstly and then increases with the increasing contact force. It increases with the increasing contact current. It increases firstly, then decreases and finally increases with the increasing sliding speed.

4) Under the same contact force, sliding speed, and current conditions, the contact current density of the friction pair under rain condition is smaller than that under no rain condition.

REFERENCES

[1] J.-G. Wang, L.-L. Feng, and Y. Li, "Influences of surface topography on electrical pitting," *J. Zhejiang Univ., Eng. Sci.*, vol. 49, no. 11, pp. 2025–2032, Nov. 2015.

[2] S. Sawada, S. Tsukiji, T. Tamai, and Y. Hattori, "Constriction current behavior of oxide film effect observed by using LED wafer," in *Proc. 26th ICEC*, Beijing, China, 2012, pp. 326–330.
[3] R. D. Malucci, "Comparison of model predictions of current density variation across simulated contact regions," in *Proc. 56th IEEE Holm Conf. Electr. Contacts*, Charleston, SC, USA, Oct. 2010, pp. 1–9.
[4] R. D. Malucci, "The impact on current density and constriction resistance from bridge structures in real contacts," in *Proc. 63rd IEEE Holm Conf. Electr. Contacts*, Denver, CO, USA, Sep. 2017, pp. 59–62.
[5] B. Swierczynski, J. J. Gonzalez, P. Teulet, P. Freton, and A. Gleizes, "Advances in low-voltage circuit breaker modelling," *J. Phys. D, Appl. Phys.*, vol. 37, no. 4, pp. 595–609, Feb. 2004.
[6] A. Omura, M. Fukuta, K. Miyake, T. Kondo, and M. Onuma, "Contact resistance of Sn-film and Sn-bulk investigated by microscopic analysis," in *Proc. 61st IEEE Holm Conf. Elect. Contacts*, San Diego, CA, USA, Oct. 2015, pp. 381–385.
[7] G. Gao, P. Xu, W. Wei, Z. Yang, and G. Wu, "The effect of running speed of high speed trains on the surface erosion of pantograph strip under pantograph arc," in *Proc. 64th IEEE Holm Conf. Elect. Contacts*, Albuquerque, NM, USA, Oct. 2018, pp. 1–5.
[8] F. Guo, X. Feng, Z. Wang, J. You, X. Wang, D. Liu, and Z. Chen, "Research on time domain characteristics and mathematical model of electromagnetic radiation noise produced by single arc," *IEEE Trans. Compon., Packag., Manuf. Technol.*, vol. 7, no. 12, pp. 2008–2017, Dec. 2017.
[9] G. B. Shang, Y. Z. Zhang, J. D. Xing, L. M. Sun, M. Qiu, Y. P. Niu, and M. Hou, "Effect of current density on surface temperature and tribology behavior of chromium bronze/brass couple," *Chin. J. Nonferrous Metals*, vol. 18, no. 7, pp. 1237–1241, Jul. 2008.
[10] L. M. Li, B. C. Jia, and G. X. Chen, "Experimental study on the factors affecting the current-receiving quality of the contact rail/collector shoe systems," *Lubrication Eng.*, vol. 33, no. 3, pp. 32–35, Mar. 2008.
[11] L. Zhou, T. C. Lu, B. Zhang, G. K. Yu, and J. W. Wan, "Multi-physics coupling analysis of rough surfaces using 3D fractal model," *Trans. China Electrotech. Soc.*, vol. 30, no. 14, pp. 226–232, Jul. 2015.
[12] W. F. Han, G. Q. Gao, X. R. Liu, S. C. Luo, G. Y. Zhu, and G. N. Wu, "MHD model of pantograph-catenary arc," *J. China Railway Soc.*, vol. 37, no. 5, pp. 21–26, May 2015.
[13] F. Y. Guo, S. Liu, and Z. Y. Wang, "Research on transient temperature field of electrical sliding contact in pantograph and catenary system," *Adv. Technol. Elect. Eng. Energy*, vol. 36, no. 3, pp. 29–34, Mar. 2017.
[14] F.-C. Duan, Z.-G. Liu, and Y. Song, "Study on the current collection of high speed pantograph-catenary system considering static wind perturbation and friction coupling," in *Proc. 35th Chin. Control Conf. (CCC)*, Chengdu, China, Jul. 2016, pp. 10236–10241.
[15] Z. Chen, G. Sun, G. Shi, and L. Hui, "Study on friction and wear of sliding electrical contact of pantograph-catenary system under fluctuating compressive load," in *Proc. 64th IEEE Holm Conf. Elect. Contacts*, Albuquerque, NM, USA, Oct. 2018, pp. 399–405.
[16] J. Zhang, W. Liu, and Z. Zhang, "Study on characteristics location of pantograph–catenary contact force signal based on wavelet transform," *IEEE Trans. Instrum. Meas.*, vol. 68, no. 2, pp. 402–411, Feb. 2019.
[17] Y. Song, Z. Liu, H. Wang, X. Lu, and J. Zhang, "Nonlinear analysis of wind-induced vibration of high-speed railway catenary and its influence on pantograph–catenary interaction," *Vehicle Syst. Dyn.*, vol. 54, no. 6, pp. 723–747, Jun. 2016.
[18] Y. Song, Z. Liu, H. Wang, J. Zhang, X. Lu, and F. Duan, "Analysis of the galloping behaviour of an electrified railway overhead contact line using the non-linear finite element method," *Proc. Inst. Mech. Eng. F, J. Rail Rapid Transit*, vol. 232, no. 10, pp. 2339–2352, Nov. 2018.
[19] *Environmental Testing for Electric and Electronic Products—Part 2: Test Methods—Test R: Water Test Method and Guidance*, Standard IEC 60068-2-18, 2017.
[20] X. R. Wang, L. H. Yang, and X. Zhang, "Study on lubrication performance of water lubricated graphite bearing," *China Sci. Technol. Inf.*, vol. 2, pp. 172–173, Oct. 2014.
[21] J. B. Luo, S. Z. Wen, and P. Huang, "Study on the relation between elastohydrodynamic lubrication and thin film lubrication conversion," *Tribology*, vol. 19, no. 1, pp. 73–78, Mar. 1999.
[22] Z. Wang, F. Guo, S. Liu, B. Baatar, Y. Wang, and H. Liang, "Temperature characteristics of sliding friction pair under high-speed and strong-current conditions," in *Proc. 63rd IEEE Holm Conf. Elect. Contacts*, Denver, CO, USA, Sep. 2017, pp. 187–193.

GUO FENGYI (Member, IEEE) was born in Inner Mongolia, China, in 1964. He received the B.S., M.S., and Ph.D. degrees in electrical engineering from Fuxin Mining Institute, Xi'an Jiaotong University, in 1987, 1990, and 1997, respectively.

He was a Visiting Professor with the University of Pretoria, from 2002 to 2003, and the University of Oxford, from 2008 to 2009. He is currently a Professor in electrical engineering with Liaoning Technical University, China. He has published more than 100 articles. His research interests include electrical contact, arc, and intelligent appliance.

GU XIN was born in Hebei, China, in 1995. She received the B.S. degree from the Faculty of Electrical and Control Engineering, Liaoning Technical University, Huludao, China, in 2017, where she is currently pursuing the M.S. degree. Her current research interests include electrical contact theory and arc.

WANG ZHIYONG was born in Liaoning, China, in 1982. He received the B.S., M.S., and Ph.D. degrees in electrical engineering from Liaoning Technical University, in 2005, 2008, and 2017, respectively. He is currently an Associate Professor with Liaoning Technical University. His research interests include electrical contact, arc, and intelligent appliance.

WANG YUTING received the B.S. and M.S. degrees in electrical engineering from Liaoning Technical University. Her current research interests are fundamental theory and application of electrical apparatus.

WANG XILI was born in 1986. He received the Ph.D. degree in mechanical engineering from Liaoning Technical University, in 2016. His research interests are mainly about application and theory of electrical apparatus.